Connecting Solvation Shell Structure to Proton Transport Kinetics
in Hydrogen–Bonded Networks via Population Correlation Functions

Amalendu Chandra,[1] Mark E. Tuckerman,[2,3] and Dominik Marx[4]

[1]*Department of Chemistry, Indian Institute of Technology, Kanpur 208016, India*
[2]*Department of Chemistry, New York University, New York, New York 10003, USA*
[3]*Courant Institute of Mathematical Sciences, New York University, New York, New York 10003, USA*
[4]*Lehrstuhl für Theoretische Chemie, Ruhr-Universität Bochum, 44780 Bochum, Germany*
(Received 28 February 2007; published 4 October 2007)

A theory based on population correlation functions is introduced for connecting solvation topologies and microscopic mechanisms to transport kinetics of charge defects in hydrogen–bonded networks. The theory is tested on the hydrated proton by extracting a comprehensive set of relaxation times, lifetimes, and rates from *ab initio* molecular dynamics simulations and comparing to recent femtosecond experiments. When applied to the controversial case of the hydrated hydroxide ion, the theory predicts that only one out of three proposed transport models is consistent with known experimental data.

Proton transfer (PT), including proton holes, and the migration of positive and negative topological charge defects in hydrogen-bonded (HB) networks, is central to a myriad of processes in chemistry, physics, materials science, and biology. *Ab initio* [1], semiempirical [2], and reactive force-field [3] simulations have elucidated many details of such structural diffusion mechanisms, yet a theory connecting a particular defect's solvation structure and microscopic PT mechanism to macroscopic charge transport kinetics is lacking. Here, a general statistical-mechanical framework that achieves the aforementioned goal within a chemical master equation (CME) approach is introduced. The theory employs the concept of population correlation functions [4] and associated rate equations [5] as commonly applied to HB kinetics but greatly extends these essential ideas in key ways, *vide infra*. Although the theory is applied here to proton transport in acids and bases, the formalism is flexible and can be straightforwardly adapted to quantify charge defect kinetics in bulk materials, at surfaces and interfaces, on soft membranes, or along water wires to name a few examples.

For simplicity, we assume all HB donors or acceptors (A) to be identical, i.e., $A - H \cdots A$; generalization to heterogeneous HBs is straightforward. Addition or removal of a proton creates a cationic or anionic defect site A^*, e.g., H_3O^+ or OH^- [see Fig. 1(a) for labeling]. We now define two charge defect population functions: $h(t) = 1$ if a tagged A atom is A^* at time t (and $h(t) = 0$ otherwise), whereas $H(t) = 1$ if A^* retains its identity continuously up to time t. These functions describe topological defect patterns as opposed to their counterparts for HB kinetics in pure liquids [4,5]. Next, we introduce an intermittent PT correlation function $C_i^{AA}(t) = \langle h(0)h(t)\rangle/\langle h\rangle$ that yields the probability of finding the same A^* at times $t = 0$ and t, irrespective of any possible identity change in the interim, and a continuous PT correlation function $C_c^{AA}(t) = \langle h(0)H(t)\rangle/\langle h\rangle$ that does not allow for any identity change of A^* in $[0, t]$. In practice, $C_i^{AA}(t)$ and $C_c^{AA}(t)$ are computed

directly from MD trajectories without explicit construction of $h(t)$ or $H(t)$.

Next, suppose there are p solvation patterns, each with a different coordination number $n_1, \ldots, n_p$. Then, $C_c^{AA}(t)$ is particularized by introducing $C_c^{AA-n_i}(t)$ describing the probability of finding the same A^* continuously up to time t given that its coordination number is n_i at time $t = 0$. Lifetimes are obtained from $\tau_{\text{exch}} = \int C_c^{AA}(t)dt$ which is the average time needed for PT from A^* to a first solvation shell member and $1/\tau_{\text{exch}}$ is the average PT rate, with an analogous definition of $\tau_{\text{exch}}^{AA-n_i}$. "Proton rattling" events, in which the defect returns to its original A^* site after two successive PTs, can be either included or excluded. Including them allows ultrafast dynamics accessible to femtosecond experiments [6] to be extracted. However, since they do not contribute to any overall net displacement, excluding them provides a clearer picture of the transport process.

The decay of $C_i^{AA}(t)$ depends not only on $1/\tau_{\text{exch}}$ but also on the reverse process. In order to disentangle the coupled forward-backward kinetics [5], a nearest-neighbor PT correlation function $C_{\text{nn}}^{AA}(t)$ is introduced which measures the probability of finding an A atom in the hydration shell of A^* at time t given that it was the A^* site at $t = 0$; analogous definitions hold for $C_i^{AA-n_i}(t)$ and $C_{\text{nn}}^{AA-n_i}(t)$. Including the reverse reaction leads to the rate equation for PT,

$$\frac{dC_i^{AA}(t)}{dt} = -k_1^{\text{PT}} C_i^{AA}(t) + k_{-1}^{\text{PT}} C_{\text{nn}}^{AA}(t), \qquad (1)$$

with k_1^{PT} and k_{-1}^{PT} being the forward and backward PT rate constants, respectively. This defines a general formalism, independent of the particular HB network, that allows the kinetics of PT and structural diffusion to be investigated theoretically in a quantitative manner. Akin to other CME approaches [7], the formalism permits one to connect long-time processes to specific microscopic motions. Further, for PT it can be established in the spirit of HB kinetics [5]
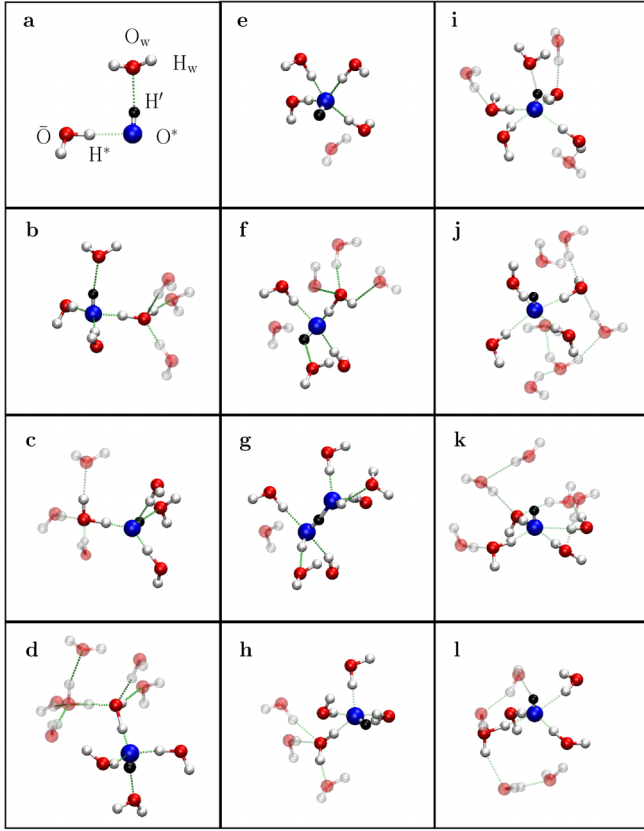
145901-1

FIG. 1 (color online). Charge migration mechanisms of $OH^-(aq)$ obtained from AIMD. Labeling convention, (a), and PW91 (b)–(d), BLYP (e)–(h), and HCTH (i)–(l) mechanisms. The most important species in the box are shown, the defect is blue and black, H_2O beyond the first shell are transparent, and the origin is fixed in space for all frames of a sequence.

that the decay properties of the intermittent and continuous correlations are directly connected via $\tilde{c}_i^{AA}(s) = \tilde{c}_c^{AA}(s) \times [1 - \tilde{n}_c^{AA}(s)]/[1 - \tilde{n}_c^{AA}(s)\tilde{c}_c^{AA}(s)]$, where $\tilde{c}_i^{AA}(s)$ and $\tilde{c}_c^{AA}(s)$ are the Laplace transforms of the probability densities $-dC_c^{AA}/dt$ and $-dC_i^{AA}/dt$, respectively, and $\tilde{n}_c^{AA}(s)$ represents the Laplace transform of the probability density for an atom A to remain as a nearest neighbor of A^* continuously in $[0, t]$ given that it was A^* before $t = 0$. Thereby, it can be shown that if $C_c^{AA}(t)$ has a biexponential decay, for example, then $C_i^{AA}(t)$ does as well, so that either function can be used for analysis.

The new theory is first tested on the transport mechanism of the hydrated proton $H^+(aq)$, which is now well understood [1]; a primitive version of this approach was recently applied to methanol-water mixtures [8]. The transport process [9,10] is linked to an interplay between a threefold coordinated complex, the "Eigen cation" $H_3O^+ \bullet (H_2O)_3$, and a shared-proton complex, the "Zundel cation" $[H_2O \cdots H \cdots OH_2]^+$ and can be rationalized in terms of the "presolvation concept" [11,12]: Prior to any PT reaction, the proton-receiving species must achieve a solvation pattern similar to the species

into which it will be transformed after the reaction. Thus, for $H^+(aq)$, a HB between the first and second solvation shell of H_3O^+ must break [9,10], thereby reducing the coordination number of a first solvation shell water molecule from four to three [9,10,13]. The rate-limiting step is the time needed for the coordination number reduction. Very recently, this predicted Grotthuss mechanism [9,10,13], including rate limitation, proton rattling, and fluxionality, was fully confirmed experimentally [6] via femtosecond vibrational spectroscopy.

Since this process involves two complexes and one essential solvation pattern the rate theory can be "closed" by a second rate equation for the conversion of a defect HB to a normal one with a rate constant k_2^{PT}:

$$\frac{dC_{nn}^{OO}(t)}{dt} = -(k_2^{PT} + k_{-1}^{PT})C_{nn}^{OO}(t) + k_1^{PT}C_i^{OO}(t). \quad (2)$$

Combined with Eq. (1), this CME rate theory can be solved analytically to yield a biexponential decay with clearly identifiable fast and slow time scales.

In order to generate trajectories, *ab initio* MD (AIMD) simulations [14] with three popular generalized gradient approximation (GGA) functionals (BLYP, PW91, and HCTH) were performed for ≈ 0.5 ns in total. From the BLYP trajectory, the decay of the computed continuous correlation function is indeed biexponential, $C_c^{OO}(t) = a_1 \exp[-t/\tau_1] + a_2 \exp[-t/\tau_2]$. Including "rattling" events, two time scales are found, $\tau_1 \approx 50$ fs and $\tau_2 \approx 260$ fs, with τ_2 partially influenced by net charge-displacement processes, and the integrated, average lifetime of the positive charge defect is $\tau_{exch} \approx 190$ fs. Furthermore, τ_1 and τ_2 can be assigned to proton rattling in Zundel-like and Eigen-like complexes, respectively. Their difference results from the location of the proton relative to the dividing surface at $|\delta| \approx 0$ Å: in Eigen-like complexes, larger amplitude vibrations and thus longer time scales are needed for the proton to return. Extracting PT rates independently from a short-time analysis of Eq. (1) yields $1/k_1^{PT} \approx 140$ fs for the short-time dynamics. Considering the various time scales, we conclude that proton rattling along HBs occurs on a time scale of roughly 50–200 fs for BLYP; PW91 and HCTH yield similar results. This finding is consistent with the time scale of <100 fs ascribed to the interconversion of Eigen and Zundel complexes in femtosecond spectroscopy [6].

Next, excluding proton rattling, the defect lifetime is $\tau_{exch} \approx 1.66$ ps which, again, is consistent with the inverse PT rate $1/k_1^{PT} \approx 1.68$ ps for true proton migration. This demonstrates that those PT events that lead to structural diffusion of the defect occur on a time scale of roughly 1–2 ps, which is an order of magnitude slower than proton rattling, but close to the HB lifetime in bulk water, $1/k_1^{HB-O_w} \approx 2$ ps; again, HCTH and PW91 lead to the same picture. Since quantum effects would accelerate the dynamics, this lifetime is in fair agreement with the experimental [17] HB lifetime of ≈ 1.4 ps. For structural

diffusion events, the corresponding experimental numbers are 1.7 or 1.3 ps (depending on experiment) and ≈ 1 ps for solvent reorganization [6]. Thus, all GGA functionals yield a consistent quantitative picture.

In stark contrast to H^+(aq), the behavior of OH^-(aq) is less clear—even controversial [9,11,12,18–21]. Using the same three GGA functionals, three different OH^-(aq) solvation patterns and transport mechanisms were obtained [12]. Pioneering studies [9] suggested that the oxygen in OH^- is on the average "hypercoordinated" [11], preferentially accepting four HBs in a roughly square-planar arrangement [see Fig. 1(e)] as confirmed later independently [22] and by neutron scattering [23]. For BLYP, the diffusion mechanism begins when OH^-(aq), itself, undergoes a coordination number reduction via the breaking of a HB between its oxygen O^* and a first-shell H_2O; Figs. 1(e) and 1(f). Next, the OH^-(aq) transiently donates one HB via its hydroxide hydrogen H', Figs. 1(f) and 1(g), leaving OH^-(aq) in a locally tetrahedral pattern. This allows facile PT, which transforms OH^- into an intact H_2O; Figs. 1(g) and 1(h). The rate-limiting step is the first-shell coordination change and the relaxation into a tetrahedral configuration.

PW91 leads to a mechanism best described by the so-called "proton-hole" picture [21]. Here, H' donates a HB but favors threefold coordination of O^*, Fig. 1(b), so that OH^- is nearly always solvated tetrahedrally, like any intact water molecule. In this arrangement, PT to OH^- readily occurs from an accepted H_2O in the first shell; Figs. 1(b) and 1(c). At the new (neighboring) site, the nascent OH^- is again perfectly coordinated and receives a proton from a neighboring H_2O; Figs. 1(c)–1(d). This mechanism yields an unphysically high structural diffusion rate [12].

For HCTH, OH^-(aq) is stably hypercoordinated; i.e., the oxygen of OH^-(aq) accepts four H_2O via HBs in a square-planar arrangement, Fig. 1(i), and preserves this coordination, thereby hindering PT from neighboring waters. Here, OH^- behaves like any inert anion with a tightly bound first solvation shell, $[OH^- \bullet (H_2O)_n]$(aq), so that diffusion is driven by second solvation shell changes due to HB fluctuations in the third shell and beyond; Figs. 1(j)–1(l). This implies that diffusion occurs hydrodynamically via the vehicular Stokes mechanism.

Using the same simulation protocol [14], the average PT rates extracted for OH^-(aq) from Eq. (1) with proton rattling excluded differ considerably for the three functionals (see Table I). PW91 and HCTH predict unphysically high and low rates, respectively, while BLYP yields a rate consistent with experiment; see Ref. [12] and referenced experimental data therein. For PW91, the decay behavior of $C_c^{OO}(t)$ is best described as triexponential yielding one slow and two fast relaxation times, τ_{slow}, τ_{fast-1}, τ_{fast-2}, with weights $a_{slow} + a_{fast-1} + a_{fast-2} = 1$. For PW91 and BLYP the fast and slow processes have relaxation times $\tau_{fast} \approx 0.5$ ps and $\tau_{slow} = 3$–4 ps, amounting to essentially 1 order of magnitude difference between the two processes. The crucial difference, how-

TABLE I. Relaxation times and inverse rates (all in ps) for OH^-(aq) excluding rattling events. The bulk HB lifetime $1/k_1^{HB-O_w}$ follows $1/k_1^{HB-O^*}$ in parentheses.

Functional	τ_{exch} $1/k_1^{PT}$	τ_{exch}^{OO-3} τ_{exch}^{OO-4}	τ_{fast-1} τ_{fast-2}	a_{fast-1} a_{fast-2}	τ_{slow} $1/k_1^{HB-O^*}$	τ_{fast}^{μ} $1/k_{-1}^{HB-H'}$
PW91	1.16	0.52	0.11	0.14	2.6	0.11
	0.74	2.50	0.66	0.52	1.9 (2.15)	0.50
BLYP	3.20	0.65	$\cdots$	0.00	4.0	0.13
	3.20	3.95	0.40	0.06	5.6 (2.20)	0.30
HCTH	15.6	$\cdots$	$\cdots$	0.00	15.0	0.15
	13.8	15.6	$\cdots$	0.00	14.0 (1.40)	0.30

ever, is the weights: the fast processes are negligible for BLYP, $a_{fast-1} + a_{fast-2} \approx 0.06$, whereas they are dominant for PW91, $a_{fast-1} + a_{fast-2} \approx 0.64$. For HCTH there is no fast process, i.e., $a_{fast-1} + a_{fast-2} \approx 0$, but $\tau_{slow} \approx 16$ ps corresponds to a dramatically slow relaxation.

Next, we consider the correlation functions $C_c^{OO-n_i}(t)$ and $C_{nn}^{OO-n_i}(t)$, introduced previously, for O^* accepting either $n_i = 3$ or 4 HBs, as defined from a distance cutoff corresponding to the first minimum of the O^*-H pair correlation. The corresponding backward rate constants are denoted $k_{-1,3}^{PT}$ and $k_{-1,4}^{PT}$. The rate equations can now be closed to yield the CME

$$\frac{dC_i^{OO}}{dt} = -k_1^{PT}C_i^{OO} + \sum_{i=1}^{p} k_{-1,n_i}^{PT}C_{nn}^{OO-n_i}$$
$$\frac{dC_{nn}^{OO-n_i}}{dt} = -(k_2^{PT} + k_{-1,n_i}^{PT})C_{nn}^{OO-n_i} + k_1^{PT}C_i^{OO}, \tag{3}$$

where $i = 1, \ldots, p$; here $p = 2$, $n_1 = 3$, $n_2 = 4$. The solution of the coupled equations can be shown to yield a triexponential decay. Comparing both τ_{exch}^{OO-4} and τ_{exch}^{OO-3} to τ_{fast-1}, τ_{fast-2} and τ_{slow}, the slow process is consistently found to be associated with PT from fourfold coordinated OH^-(aq) since $\tau_{slow} \approx \tau_{exch}^{OO-4}$ for all three functionals (see Table I). Yet, it is τ_{exch}^{OO-3} and thus the threefold coordinated OH^-(aq) species that can be linked exclusively to the fast processes. Indeed, the relations $\tau_{fast} \approx \tau_{exch}^{OO-3} \ll \tau_{exch}^{OO-4} \approx \tau_{slow}$ strongly support our mechanistic picture derived from the presolvation concept: PT occurs preferentially if the proton-receiving species is properly solvated, independent of the functional and its predicted mechanism.

In order to connect these different time scales to underlying microscopic dynamics, the lifetimes of HBs between the defect O^* and first-shell solvation water only, $1/k_1^{HB-O^*}$, were computed. Here, the three time scales $1/k_1^{HB-O^*}$, τ_{slow}, and τ_{exch}^{OO-4} are similar for each functional (see Table I), consistent with the idea that fluctuations of HBs between OH^- and water molecules in its first shell drive structural diffusion for BLYP and HCTH. For HCTH, however, this HB lifetime is unusually long, $1/k_1^{HB-O^*} \gg 1/k_1^{HB-O_w}$, implying that the first shell is very tightly bound to OH^- and hydrodynamic diffusion dominates.

For PW91, in stark contrast, the two HB lifetimes far exceed the fast relaxation times, i.e., $1/k_1^{\mathrm{HB-O}_w} \approx 1/k_1^{\mathrm{HB-O}^*} \gg \tau_{\mathrm{fast-1}}, \tau_{\mathrm{fast-2}}$. The previous finding that fast relaxation is the dominant channel to PT for PW91 by about 60% implies that another process must correlate with PT. This is identified to be the short-time component of water reorientational motion in the first solvation shell of OH$^-$ since this time scale, denoted τ_{fast}^μ (Table I), matches only the ultrafast PT component $\tau_{\mathrm{fast-1}}$. Furthermore, when the rate for HB formation involving H$'$ of OH$^-$(aq), $k_{-1}^{\mathrm{HB-H}'}$ is computed we find that it matches $\tau_{\mathrm{fast-2}}$ for PW91 and BLYP in Table I; note that HCTH features only a slow channel to PT, τ_{slow}. Thus, if the donated HB is formed by OH$^-$(aq) through the OH$^-$ hydrogen, H$'$, then PT is triggered by ultrafast rotational or reorientational motion of solvation water; otherwise this H$' \cdots$O$_w$ HB needs to be formed first for proper pre-solvation before PT can occur. This analysis naturally explains "...why the simulation rates are higher than observed experimental rates" [21] for OH$^-$(aq) with PW91.

The full picture is obtained by including proton rattling: Table II shows that the associated time scale, for all functionals, is considerably faster when OH$^-$ accepts three HBs in comparison to fourfold coordination since $\tau_{\mathrm{exch}}^{\mathrm{OO-4}} \gg \tau_{\mathrm{exch}}^{\mathrm{OO-3}}$. Interestingly, we find that the slow time scale τ_{slow}, for all functionals, matches the time $\tau_{\mathrm{exch}}^{\mathrm{OO-4}}$ that fourfold coordinated species spend on average without any PT, be it rattling or actual charge migration (i.e., PW91: 0.60 vs 0.54, BLYP: 1.70 vs 1.55, HCTH: 1.76 vs 1.80). Most important is the observation that for PW91 only, the two time scales τ_{fast} and τ_{slow} (i.e., 0.06 and 0.60) are essentially identical to $\tau_{\mathrm{fast-1}}$ and $\tau_{\mathrm{fast-2}}$ (i.e., 0.11 and 0.66) found for real PT and thus structural diffusion (see Table I). This crucial finding implies that for PW91 only, rattling and structural diffusion must occur on the same time scale.

Concerning the current controversy, our findings suggest that "spectral tagging" experiments of the sort used for acids [6] could uncover the true nature of basic aqueous solutions, including the origin of the $\sim$160 fs time scale [24] (cf. Table II). The good quality of the fit of the MD data to the kinetics model indicates a separation between

the ultrafast local proton transfer and long-range proton transport modes, although the model does not require that associated mode variables be explicitly identified. In general terms, the quantitative connection of local proton transfer to long-range proton transport provided by our theoretical framework is expected to open up wide applications to understand a host of diverse phenomena such as, e.g., proton conductivity in fuel cells or vectorial proton transport through biomembranes.

[1] D. Marx, Chem. Phys. Chem., **7**, 1848 (2006).
[2] G. A. Voth, Acc. Chem. Res. **39**, 143 (2006).
[3] B. Roux, Acc. Chem. Res. **35**, 366 (2002).
[4] F. H. Stillinger, Adv. Chem. Phys. **31**, 1 (1975); D. C. Rapaport, Mol. Phys. **50**, 1151 (1983).
[5] A. Luzar and D. Chandler, Nature (London) **379**, 55 (1996); A. Luzar, J. Chem. Phys. **113**, 10 663 (2000).
[6] S. Woutersen and H. J. Bakker, Phys. Rev. Lett. **96**, 138305 (2006).
[7] J. D. Chodera et al., J. Chem. Phys. **126**, 155101 (2007).
[8] J. A. Morrone et al., J. Phys. Chem. B **110**, 3712 (2006).
[9] M. E. Tuckerman et al., J. Phys. Chem. **99**, 5749 (1995); J. Chem. Phys. **103**, 150 (1995).
[10] N. Agmon, Chem. Phys. Lett. **244**, 456 (1995).
[11] M. E. Tuckerman et al., Nature (London) **417**, 925 (2002).
[12] M. E. Tuckerman et al., Acc. Chem. Res. **39**, 151 (2006).
[13] D. Marx et al., Nature (London) **397**, 601 (1999).
[14] AIMD [15,16] was performed using a 9.865 Å box, 32 H$_2$O with one excess or missing H$^+$, and the BLYP, PW91, and HCTH/120 functionals. For BLYP and HCTH, Troullier-Martins pseudopotentials with a cutoff of 70 Ry, and for PW91, ultrasoft pseudopotentials with 30 Ry, were employed. The D mass was used instead of H to minimize quantum effects with a fictitious electron mass of 800 a.u. and a 5 a.u. time step. Each system was carefully equilibrated at 300 K for 10–15 ps followed by 20–50 ps of microcanonical dynamics each.
[15] R. Car and M. Parrinello, Phys. Rev. Lett. **55**, 2471 (1985).
[16] J. Hutter et al., CPMD, see www.cpmd.org.
[17] C. J. Fecko et al., J. Chem. Phys. **122**, 054506 (2005).
[18] N. Agmon, Chem. Phys. Lett. **319**, 247 (2000).
[19] Z. W. Zhu and M. E. Tuckerman, J. Phys. Chem. B **106**, 8009 (2002).
[20] R. Ludwig, Angew. Chem., Int. Ed. **42**, 258 (2003).
[21] D. Asthagiri et al., Proc. Natl. Acad. Sci. U.S.A. **101**, 7229 (2004).
[22] P. Vassilev et al., J. Phys. Chem. B **109**, 23605 (2005).
[23] A. Botti et al., J. Chem. Phys. **119**, 5001 (2003); S. Imberti et al., J. Chem. Phys. **122**, 194509 (2005).
[24] H.-K. Nienhuys et al., J. Chem. Phys. **117**, 8021 (2002).

TABLE II. Relaxation times and inverse rates (all in ps) for OH$^-$(aq) including rattling events.

Functional	τ_{exch} $1/k_1^{\mathrm{PT}}$	$\tau_{\mathrm{exch}}^{\mathrm{OO-3}}$ $\tau_{\mathrm{exch}}^{\mathrm{OO-4}}$	τ_{fast} a_{fast}	τ_{slow} a_{slow}
PW91	0.27	0.08	0.06	0.60
	0.09	0.54	0.61	0.39
BLYP	1.35	0.16	0.18	1.70
	0.59	1.55	0.20	0.80
HCTH	1.78	$\cdots$	$\cdots$	1.76
	1.65	1.80	0.00	1.00